Materials Today: Proceedings 48 (2022) 1899–1904

Contents lists available at ScienceDirect

Materials Today: Proceedings

journal homepage: www.elsevier.com/locate/matpr

Nanocellulose from oil palm mesocarp fiber using hydrothermal treatment with low concentration of oxalic acid

N.F. Abu Bakar [a], N. Abd Rahman [a,*], M.B. Mahadi [a], S.A. Mohd Zuki [a], K.N. Mohd Amin [b], M.Z. Wahab [c], I. Wuled Lenggoro [d,e,f]

[a] School of Chemical Engineering, College of Engineering, Universiti Teknologi MARA, 40450 Shah Alam, Selangor, Malaysia
[b] Faculty of Chemical and Process Engineering Technology, Universiti Malaysia Pahang, Lebuh Raya Tun Razak, Gambang, Pahang 26300, Malaysia
[c] B4, Bangunan Kilang Tabung Haji, Jalan Gebeng 3/2, Kawasan Industri Gebeng, 26080 Kuantan, Pahang, Malaysia
[d] Graduate School of Bio-Applications and Systems Engineering, Tokyo University of Agriculture and Technology (TUAT), 2-24-16, Naka-cho, Koganei-shi, Tokyo 184-8588, Japan
[e] Department of Applied Physics and Chemical Engineering, TUAT, 2-24-16, Naka-cho, Koganei-shi, Tokyo 184-8588, Japan
[f] Institute of Global Innovation Research, TUAT, 3-8-1 Harumi-cho, Fuchu-shi, Tokyo 183-8538, Japan

ARTICLE INFO

Article history:
Available online 13 October 2021

Keywords:
Hydrothermal treatment
Oil palm mesocarp fiber
Oxalic Acid Dihydrate
Nanocellulose

ABSTRACT

Nanocellulose from oil palm mesocarp fiber (OPMF) was isolated using hydrothermal treatment at a pressure of 150 kPa and 120 °C coupled with hydrolysis of low concentration of weak acid i.e. oxalic acid dihydrate (OAD). Two different concentrations of OAD i.e. 11 and 13 wt% were introduced in the acid hydrolysis process. Crystallinity index of the raw fiber increased from 39.5 to 70.4 and 70% for 11 and 13 wt% OAD, respectively. The average particles sizes of nanocellulose measured using TEM was approximately 25 nm for both concentrations of OAD which approximately equivalent to the one measured using dynamic light scattering (DLS). The values of zeta potential of the nanocellulose suspension isolated using 11 and 13 wt% OAD were −26 and −27.5 mV respectively. Isolation technique which is hydrothermal treatment coupled with low concentration of OAD was effective in producing OPMF nanocellulose at high crystallinity index, less than 100 nm size distribution, and it is a stable suspension.

1. Introduction

Palm oil production is one of the major agricultural crops that contribute to the economic growth of Malaysia. Current policy of Malaysia aims to produce 23% of oil extraction recovery in the oil palm milled industry whereby biomass generated is expected to increase from 80 million tonnes in 2010 to 110 million tonnes in 2020. The biomass generated includes oil palm empty fruit bunches (OPEFB), palm kernel shell (PKS), oil palm mesocarp fiber (OPMF), palm oil mill effluent (POME), oil palm trunk (OPT), oil palm leaves (OPL) and oil palm frond (OPF). Oil palm mesocarp fiber (OPMF) is one of the biomasses produced after an extraction of crude palm oil. The OPMF are usually used as fuel to generate steam for boiler. The boiler is used in sterilization process of fresh fruit bunch (FFB). Oil content of the OPMF should be below than 6% after being pressed by screw press to obtain palm oil. It contains 42.81–32.22% of cellulose, 33.10–31.62% of hemicellulose and 20.49–23.89% of lignin [1]. It also creates a big opportunity for researchers as it is rich in lignocellulose which is highly potential of nanocellulose development for further application [2,3].

Nanocellulose is a result of an isolation process from plant and generally referred as cellulose in nanosizes [4]. Several advantages of nanocellulose that have already been discovered, are biodegradable, renewable resources, high specific strength and modulus. Nanocellulose can be categorized into two types which are filament- like cellulose nano fibrils (CNF) or rod-like cellulose nanocrystals (CNC) [5,6]. Width of CNF is between 5 and 60 nm and a length of about several micrometers, whereas the width and length of CNC is around 5–70 nm and 100–250 nm respectively. CNF and CNC are obtained via mechanical disintegration methods such as ultrasonication and homogenization, steam explosion [7,8], superheated steam [9], cryo-crushing, aqueous counter collision, nanofibrillation [10] or milling in combination with biological and/or chemical pretreatments [11,12] or produced

* Corresponding author.
E-mail addresses: fitrah@uitm.edu.my (N.F. Abu Bakar), noraz695@uitm.edu.my (N. Abd Rahman).

https://doi.org/10.1016/j.matpr.2021.09.357
2214-7853/

via acid hydrolysis, enzymatic treatment, hydrothermal treatment, ultrasonication [13] or combinations thereof [14,15]. Few researches have been conducted on OPMF to isolate nanocellulose. Recent work demonstrates the isolation and characterization of nanocellulose from OPMF using sulphuric acid during hydrolysis of the cellulose [16]. They produce nanocellulose from OPMF using strong acid hydrolysis with maximum 70% of crystallinity index and average diameter of 7–21 nm.

An alternative way to replace the usage of strong acid is by introducing weak acid such as oxalic acid which is important to reduce environmental issues during the process. Oxalic acid is an organic acid usually found in plants. The acid is a type of weak and dicarboxylic acid. Oxalic acid has a low water solubility at ambient temperature and thus, it can be crystallized by using low cost acid recovery [17]. Previous studies used 11% concentration of oxalic acid in acid hydrolysis to isolate nanocellulose from banana and pineapple leaf fibers by using an autoclave [18]. Crystallinity obtained were 73.62 and the diameter of the nanocellulose obtained was around 5–60 nm respectively. This shows a great opportunity to use 11% concentration of oxalic acid by combining with an autoclave. Standard solubility of oxalic acid is 143 g/L which is 14% wt/v concentration. Oxalic acid dihydrate is 71% purity from anhydrous oxalic acid. It is more stable than anhydrous because it contains two molecules of water.

Objective of this study is to isolate nanocellulose from OPMF using hydrothermal treatment coupled with low concentration of weak acid i.e. 11 and 13 wt% of oxalic acid dihydrate (OAD). Compare to sulfuric acid, OAD can be easily recycle as it has low water solubility at ambient temperature and can be crystalized easily for acid recovery [19]. To the knowledge of authors, this is the first application of using OAD as a weak acid for isolating nanocellulose of waxed and oily lignocellulosic sample of OPMF. As OPMF is an oily lignocellulosic biomass, efficiency of cellulose isolation will decrease as oil content hinders chemical to get through into the OPMF component (lignin, hemicellulose and cellulose)

2. Materials and method

Oil Palm Mesocarp Fiber (OPMF) was obtained from Felda Sungai Tengi (Selangor, Malaysia). Chemical reagents used were oxalic acid dihydrate (OAD) (purchased from Sigma - Aldrich, USA), sodium hypochlorite solution, glacial acetic acid and sodium hydroxide (purchased from R&M Chemical, Malaysia).

2.1. Materials

Oil Palm Mesocarp Fiber (OPMF) was obtained from Felda Sungai Tengi (Selangor, Malaysia). Chemical reagents used were oxalic acid dihydrate (OAD) (purchased from Sigma - Aldrich, USA), sodium hypochlorite solution, glacial acetic acid and sodium hydroxide (purchased from R&M Chemical, Malaysia).

2.2. Isolation of nanocellulose

Isolation of cellulose was modified from methodology by [18,20]. OPMF were dried in an oven at 105 °C for 1 day. Then, the dried OPMF was grinded using a cutting mill and sieved using 500 μm sieve. The milled OPMF were treated using 4 wt% (w/v) NaOH at 121 °C for 1 hr by using an autoclave. Alkali treatment was repeated twice. Then, bleaching treatment was carried out using a mixture of NaOH and acetic acid (27 g and 75.1 mL respectively) and a mixture of 1:3 vol of sodium hypochlorite solutions. The bleaching was set at 70 °C for 2 hrs. The ratio of fiber to liquor was 10:100 (g/mL). Bleaching step was repeated until the sample turned white. The bleached samples were washed with distilled water and filtered using filter paper after each treatment.

The bleached fibers were treated using autoclave as a hydrothermal treatment technique coupled with hydrolysis using OAD. The autoclave was set to a pressure and temperature setting of 150 kPa and 121 °C, respectively for 1 hr. The samples were hydrolyzed using two different concentrations of OAD i.e. 11 and 13 wt%. The pressure was released immediately after 1 h. The fibers were then subjected to dialysis using cellulose tubing membrane until pH turn to 7. The fibers were then sonicated using an ultrasonicator at an output of 700 W, frequency of 20 kHz and amplitude of 20% for 15 min. Then, it was freeze-dried to remove the water and recover the nanocellulose in solid phase only. The process is illustrated as in Fig. 1.

2.3. Characterization

2.3.1. Fourier transform infrared spectroscopy (FTIR)

FTIR spectra for raw, bleached and isolated OPMF were recorded using FTIR (Perkin Elmer, US) within a range of 500–4000 cm^{-1} to examine the changes in their functional groups due to the treatment used.

2.3.2. X-ray diffraction (XRD) analysis

Crystallinity index of nanocellulose was determined using X-Ray Diffraction (XRD, Rigaku Ultima IV, Japan) at 40 kV and 40 mA. Samples were scanned in the range of 2θ from 10 to 50° with a scanning rate of 2°/min at room temperature. Major intensity peak is located around 22.6° which indicate the crystalline structure of cellulose whilst around 18° refer to the amorphous region [21]. Crystallinity index (CrI) of cellulose has been calculated using Segal's empirical formula [21];

$$CrI = \frac{I_{002} - I_{am}}{I_{002}} \times 100$$

where, CrI is crystallinity index of cellulose, I_{002} is intensity of lattice peak diffraction and I_{am} is intensity of the amorphous fraction.

2.3.3. Field emission scanning electron microscope (FESEM)

Morphology and size reduction of raw, bleached and isolated OPMF (nanocellulose) samples were determined using FESEM (Carl Zeiss AG, Germany) at 15 kV.

2.3.4. Transmission electron microscopy (TEM)

TEM was used to study structure and size of nanocellulose produced from OPMF. The samples were analyzed using TEM (Tecnai G2 F20 X-Twin, US). Aspect ratio, L/D of nanocellulose was calculated from captured images where L and D is length and width of 100 selected nanocellulose respectively.

2.3.5. Particle size and zeta potential values

Particle size distribution using dynamic light scattering (DLS) and zeta potentials of OPMF nanocellulose were measured using Zetasizer Analyzer (Nano ZS, Malvern, UK) at pH 7. Deionised water was used as a dispersant. Three replicated data were recorded.

3. Results and discussion

3.1. FTIR

Figure 2 shows spectra analysis of FTIR for raw, bleached and isolated OPMF using 11 and 13 wt% OAD. 11 and 13 wt% OAD is considered as low concentration since in previous research, 50% concentration of oxalic acid [22] was used. Furthermore, this research used oxalic acid dihydrate which has 71% purity i.e lower than anhydrous oxalic acid. The main lignin peaks can be found at 2922 cm^{-1}, 2845 cm^{-1} [16]. The bleached and isolated OPMF shows lower spectral intensity than the raw fiber due to removal

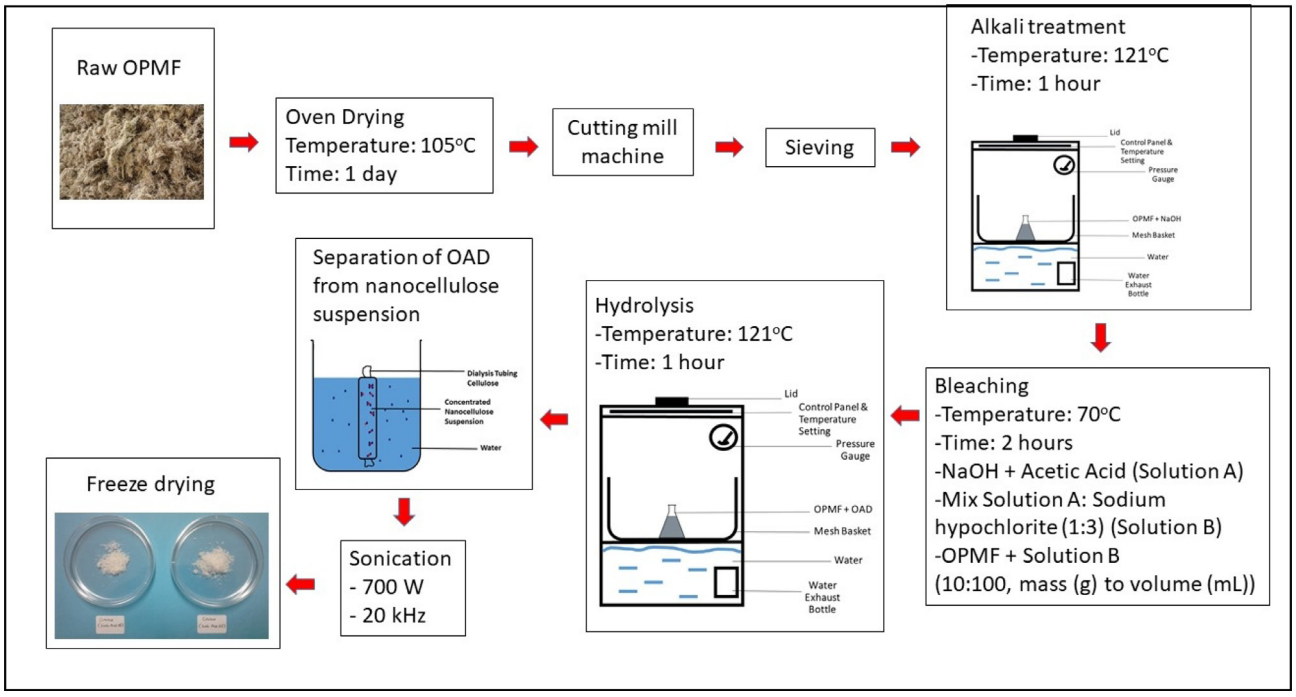

Fig. 1. Illustrative diagram for the isolation of nanocellulose from OPMF.

of hemicellulose and lignin fractions during processing. Raw fiber shows an intense peak at 1705 cm^{-1} that indicates ester linkage of carboxylic group of ferulic and p-coumaric acids of lignin or hemicelluloses. The peak between 1701 and 1731 cm^{-1} is attributed to C = O stretching of hemicellulose and lignin [16,23]. Moreover, these peaks were less visible in the spectra of the bleached fiber and hydrolyzed fibers due to removal of lignin and hemicellulose by chemical treatments [16]. This result strongly agreed with [24] which indicates that wax and oil covered the external surface of the fiber cell wall was removed with an alkali treatment. However, a peak is observed at 1702 cm^{-1} for nanocellulose (isolated OPMF) which reflected esterification process of ester carbonyl group (C = O) that occurred during acid hydrolysis process using OAD. The peak indicated a weak intensity which can be concluded as weak degree of esterification [22]. The absorption band at 897–1160 associated with cellulose [23,25] due to C–O stretching and C–H rocking appears in the spectra of raw, bleached, isolated OPMF of 11 and 13 wt% OAD which originated from OPMF.

3.2. XRD analysis

XRD patterns of raw, bleached and isolated OPMF (nanocellulose) are shown in Fig. 3. All samples exhibited high peak intensity at 2θ value of 21-22° related to crystalline structure of cellulose. A broad peak at around 15° indicates amorphous arrangement of OPMF which is a crystalline polymorph I cellulose [5]. The high intensity peak at 2θ = 22° for bleached OPMF was representing high composition of crystal structure of the fiber. Crystallinity

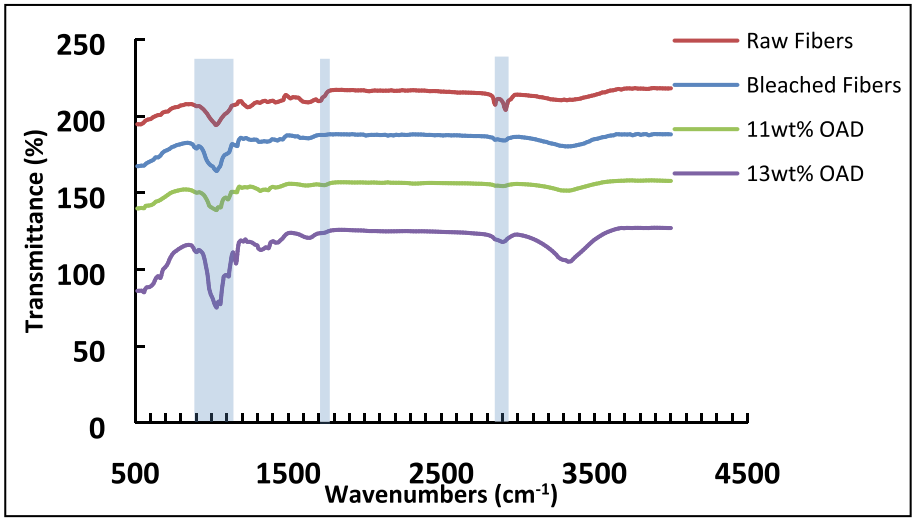

Fig. 2. FTIR bands for raw, bleached, isolated OPMF with 11wt% and 13 wt% OAD.

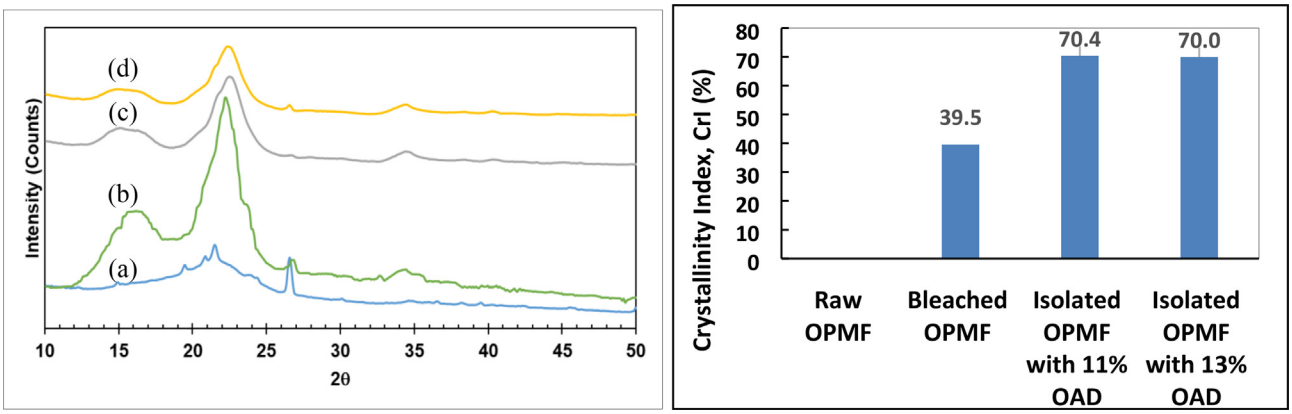

Fig. 3. XRD analysis and crystallinity index of fibers (a) raw OPMF, (b) bleached OPMF, (c) isolated OPMF with 11 wt% OAD and (d) isolated OPMF with 13 wt% OAD.

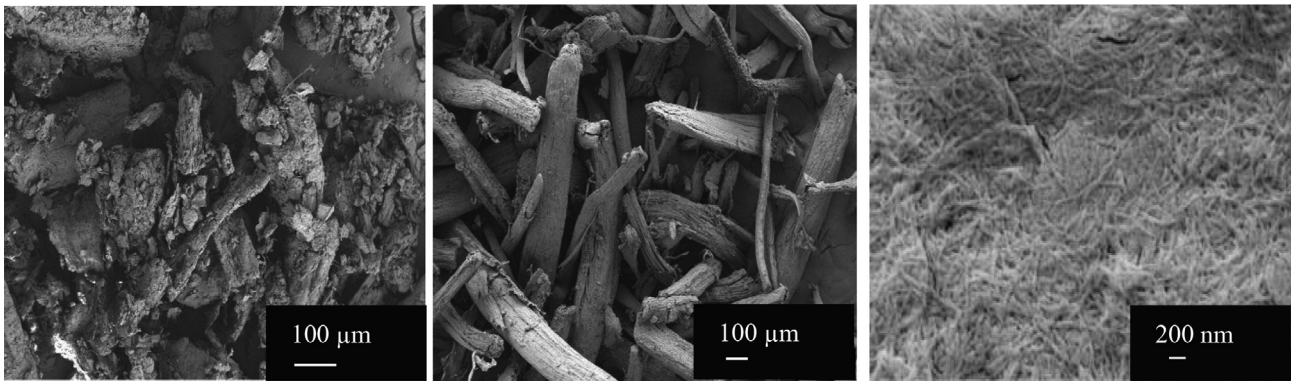

Fig. 4. FESEM images of OPMF (a) raw, (b) bleached and (c) isolated (nanocellulose before sonicating).

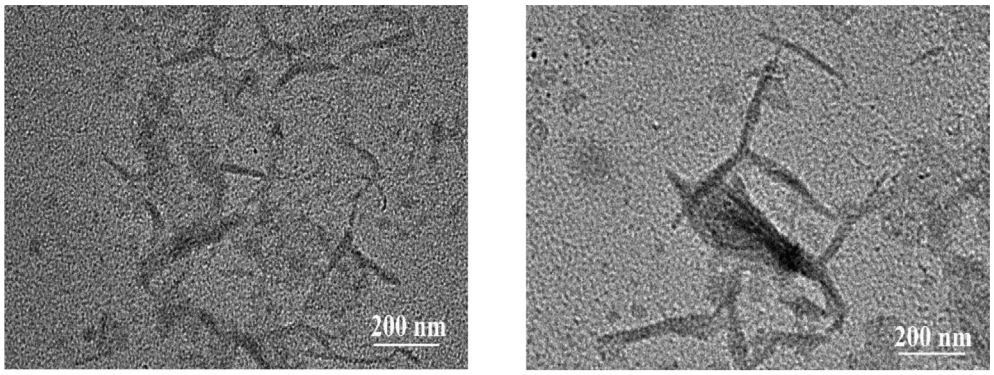

Fig. 5. TEM images of nanocelluloses from isolated OPMF for (a) 11 wt% and (b) 13 wt% OAD.

index (CrI) of the isolated OPMF increased from 39.5% for the raw fiber to 70.4 and 70.0% for 11 and 13 wt% OAD respectively. Increasing value of CrI showed that hydrothermal treatment and acid hydrolysis successfully removed lignin and hemicelluloses that were attached to the cellulosic fibers. The CrI of nanocellulose in this research is lower than the isolated OPMF by [20] i.e. 77.8% where OPMF is isolated using 65 wt% sulphuric acid. However, the value of CrI in this research is remarkable since the concentration of OAD used is very low which is 11 and 13 wt%. It is proved that by using hydrothermal treatment and coupled with low concentration of weak acid (OAD), the CrI value of OPMF is comparable and as good as the one that used concentrated and strong acid. On the other hand, the CrI value of the produced isolated OPMF nanocellulose is higher than the one using pulverized Kenaf core particle [26] although the same process was applied.

3.3. Field emission scanning electron microscope (FESEM)

Figure 4 shows FESEM images of raw, bleached and isolated OPMF (before sonication process). Raw OPMF exhibited irregular surface and some residues from grinding activities. After bleaching, the residues disappeared as shown in Figure 4(b) . Figure 4 (c) shows the FESEM image of the isolated OPMF (nanocellulose) where the nanocellulose, which was in flaky structure, were still intact. Results suggested the removal of hemicellulose and lignin occurred during hydrothermal treatment and hydrolysis.

3.4. Transmission electron microscopy (TEM)

Figure 5(a) and (b) show TEM images for 11 and 13 wt% OAD of nanocellulose produced after ultrasonication. The images showed a

disordered elongated rice-like of nanocellulose which can be considered as CNC as highlighted by Moon et al. [27]. Nanocellulose can be isolated into filament-like cellulose nanofibres which is CNF or rod-like or elongated rice-like cellulose nanocrystals (CNC) [27]. Fig. 5 indicates that hydrothermal treatment of bleached OPMF using OAD produced a nano scale of a disordered elongated rice-like shape of nanocellulose. Acid treatment was expected to remove amorphous region and maintain a flat crystal region of cellulose under controlled condition. Average value of width and length of both samples are shown in Table 1. Calculated length, width and aspect ratio of the nanoparticles are 263.32 ± 80. 12 nm, 24.80 ± 7.33 nm and 5–25 for 11 wt% OAD respectively and 256.24 ± 88.77 nm, 24.56 ± 8.64 nm and 5–27 for 13 wt% OAD respectively.

3.5. Zeta potential and DLS measurements

Table 1 shows zeta potential values around −26.0 and −27.5 mV for 11 and 13 wt% OAD respectively which shows high stability of nanocellulose suspension due to abundant natural hydroxyl groups on surface of the nanocellulose crystal. However, reported zeta potential values were lower than the one found by [28] where OPMF zeta potential values may induce agglomeration. Therefore, agglomeration of nanocellulose was expected and observed in Fig. 6. Fig. 6 shows cumulative particle size distribution (PSD) for nanocellulose OPMF isolated using 11 and 13 wt% OAD. It has been observed that lack of surface charge i.e. less than 30 mV induced continuing agglomerate of insoluble nanocellulose particles, resulted in a wide and binomial size distribution. Diameter of the nanocellulose was taken as approximately 25 nm. The finding is in agreement with the results from TEM images as depicted in Table 1. Particle size distribution for 13 wt% OAD with 25 nm diameter was lower than 11 wt% OAD. It was due to high agglomeration found at 51 nm where high concentration of acid during hydrolysis produced small size of nanocellulose of isolated OPMF that can be easily agglomerated.

Table 1
Dimension and zeta potential of isolated OPMF (nanocellulose).

Sample	Length (nm) (based on TEM images)	Width (nm) (based on TEM images)	Aspect ratio	pH	Zeta Potential (mV)
11 wt% OAD	263.32 ± 80.12	24.80 ± 7.33	5–25	7.0	−26.0
13 wt% OAD	256.24 ± 88.77	24.56 ± 8.64	5–27	7.0	−27.5

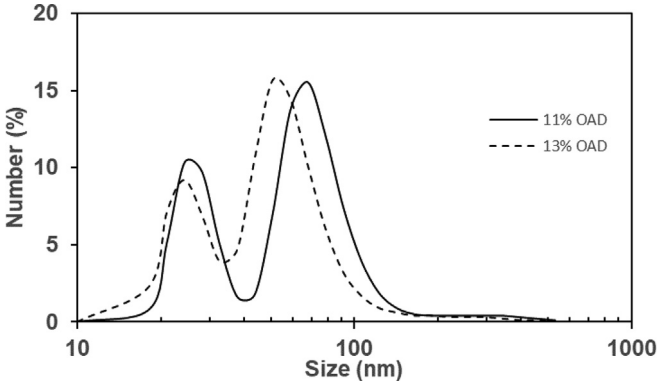

Fig. 6. Particle size distribution of isolated OPMF using 11 wt% and 13wt% OAD.

4. Results and discussion

Isolation of nanocellulose from oil palm mesocarp fiber (OPMF) has been successfully achieved by using a combination of hydrothermal treatment and weak acid hydrolysis i.e. oxalic acid dihydrate (OAD). Nanocellulose produced from this method with 11 wt% and 13wt% OAD show rod-like morphology with an aspect ratio around 5 to 25 and 5 to 27 respectively and diameter (width) of approximately 25 nm. It has higher crystalline index as compared to raw fiber and it is a stable nanocellulose suspension. With crystallinity index (CrI) around 70%, the proposed technique using hydrothermal treatment and coupled with weak acid hydrolysis at low concentration shows potential application in isolating nanocellulose for OPMF biomass. This technique is potential to be applied for isolating other lignocellulosic biomass in the future.

CRediT authorship contribution statement

N.F. Abu Bakar: Funding acquisition, Supervision, Validation, Writing original draft, Writing – review & editing. **N. Abd Rahman:** Conceptualization, Data curation, Supervision, Validation, Visualization, Writing – review & editing. **M.B. Mahadi:** Data curation, Formal analysis, Investigation, Writing – original draft. **S.A. Mohd Zuki:** Investigation, Methodology, Writing – review & editing. **K. N. Mohd Amin:** Methodology, Validation, Writing – review & editing. **M.Z. Wahab:** Resources, Writing – review & editing. **I. Wuled Lenggoro:** Validation, Visualization, Writing – review & editing.

Declaration of Competing Interest

The authors declare that they have no known competing financial interests or personal relationships that could have appeared to influence the work reported in this paper.

Acknowledgements

The authors acknowledge Universiti Teknologi MARA (UiTM) for funding this work. This study was supported by BESTARI grant from Universiti Teknologi MARA (UiTM) 600-IRMI/ MyRA 5/3/BESTARI (021/2017) and 100-TNCPI/GOV 16/6/2 (033/2020).

References

[1] R.T. Oğulata, H.İ. İçOğLu, J. Text. Inst. 106 (2015) 57–66.
[2] S.A. Mohd Zuki, N. Abd Rahman, N.F. Abu Bakar, IOP Conf. Ser. Mater. Sci. Eng. (2018).
[3] S. Saallah, M. Misson, S. Siddiquee, J. Roslan, M.N. Naim, N.F.A. Bakar, I.W. Lenggoro, Compos. Mater. Appl. Eng. Biomed. Food Sci. (2020) 369–385.
[4] M.B. Mahadi, N.A. Rahman, S.F.A. Manaf, J. Teknol. 76 (2015) 37–41.
[5] K.N.M. Amin, N. Amiralian, P.K. Annamalai, G. Edwards, C. Chaleat, D.J. Martin, Chem. Eng. J. 302 (2016) 406–416.
[6] M.G. Thomas, E. Abraham, P. Jyotishkumar, H.J. Maria, L.A. Pothen, S. Thomas, Int. J. Biol. Macromol. 81 (2015) 768–777.
[7] M. Mahardika, H. Abral, A. Kasim, S. Arief, M. Asrofi, Fibers 6 (2018) 1–12.
[8] N. Manhas, K. Balasubramanian, P. Prajith, P. Rule, S. Nimje, RSC Adv. 5 (2015) 23999–24008.
[9] M.N.F. Norrrahim, H. Ariffin, T.A.T. Yasim-Anuar, F. Ghaemi, M.A. Hassan, N.A. Ibrahim, J.L.H. Ngee, W.M.Z.W. Yunus, Cellul. 2018 257 25 (2018) 3853–3859.
[10] T.A.T. Yasim-Anuar, H. Ariffin, M.N.F. Norrrahim, M.A. Hassan, T. Tsukegi, H. Nishida, J. Clean. Prod. 207 (2019) 590–599.
[11] H.P.S. Abdul Khalil, Y. Davoudpour, M.N. Islam, A. Mustapha, K. Sudesh, R. Dungani, M. Jawaid, Carbohydr. Polym. 99 (2014) 649–665.
[12] O. Nechyporchuk, M.N. Belgacem, J. Bras, Ind. Crops Prod. 93 (2016) 2–25.
[13] T.A.T. Yasim-Anuar, H. Ariffin, M.A. Hassan, IOP Conf. Ser. Mater. Sci. Eng. 368 (2018).
[14] K.N. Mohd Amin, P.K. Annamalai, I.C. Morrow, D. Martin, RSC Adv. 5 (2015) 57133–57140.
[15] J. Prasad Reddy, J.W. Rhim, Mater. Lett. 129 (2014) 20–23.
[16] A. De Campos, A.R. De Sena Neto, V.B. Rodrigues, V.A. Kuana, A.C. Correa, M.C. Takahashi, L.H.C. Mattoso, J.M. Marconcini, J. Nanosci. Nanotechnol. 17 (2017) 4970–4976.

[17] L. Chen, B. Carlo, J.Y. Zhu, P. Kiti, Thomas Elder, Green Chem. 5–7 (2016).
[18] B.M. Cherian, A.L. Leão, S.F. de Souza, S. Thomas, L.A. Pothan, M. Kottaisamy, Carbohydr. Polym. 81 (2010) 720–725.
[19] K. Kafle, K. Greeson, C. Lee, S.H. Kim, Text. Res. J. 84 (2014) 1692–1699.
[20] B.W. Chieng, S.H. Lee, N.A. Ibrahim, Y.Y. Then, Y.Y. Loo, Polymers (Basel) 9 (2017) 1–11.
[21] L. Segal, J.J. Creely, A.E. Martin, C.M. Conrad, Text. Res. J. 29 (1959) 786–794.
[22] L. Chen, J.Y. Zhu, C. Baez, P. Kitin, T. Elder, Green Chem. 18 (2016) 3835–3843.
[23] Y. Okahisa, Y. Furukawa, K. Ishimoto, C. Narita, K. Intharapichai, H. Ohara, Carbohydr. Polym. 198 (2018) 313–319.
[24] E. Abraham, B. Deepa, L.A. Pothan, M. Jacob, S. Thomas, U. Cvelbar, R. Anandjiwala, Carbohydr. Polym. 86 (2011) 1468–1475.
[25] S. Palamae, P. Dechatiwongse, W. Choorit, Y. Chisti, P. Prasertsan, Carbohydr. Polym. 155 (2017) 491–497.
[26] S.A.M. Zuki, S.A.M. Zuki, M.S. Bin Azman, N.A. Rahman, N.F.A. Bakar, Int. J. Eng. Technol. 7 (2018) 311–315.
[27] R.J. Moon, A. Martini, J. Nairn, J. Simonsen, J. Youngblood, Cellulose Nanomater. Rev.: Struct. Properties Nanocompos. (2011).
[28] S. Rashid, A. Kumar Shahi, H. Dutta, J. Kumar Sahu, Biointerface Res. Appl. Chem. 12 (2022) 1705–1720.